ORIGINAL RESEARCH

The Inferior Cerebellar Peduncle Sign: A Novel Imaging Marker for Differentiating Multiple System Atrophy Cerebellar Type from Spinocerebellar Ataxia

Chae Young Lim[1], Yujin Seo[1], Beomseok Sohn[1], Minjung Seong[1], Sung Tae Kim[1], Sungjun Hong[2,3], Jinyoung Youn[4,5], Eung Yeop Kim[1]

ABSTRACT

BACKGROUND AND PURPOSE: The hot cross bun (HCB) sign is a hallmark feature of multiple system atrophy with predominant cerebellar ataxia (MSA-C), typically observed in advanced stages of the disease; however, it can also present in other conditions such as spinocerebellar ataxia (SCA), making the differentiation challenging. The middle cerebellar peduncle (MCP) sign may be observed in various medical conditions and in healthy individuals. We hypothesized that the inferior cerebellar peduncle (ICP), known to be affected in MSA-C, may exhibit hyperintensity on fluid-attenuated inversion recovery (FLAIR) imaging, potentially aiding in differentiating MSA-C from SCA.

MATERIALS AND METHODS: Medical records of 153 probable MSA-C and 72 genetically confirmed SCAs from a single institution were reviewed retrospectively between January 2012 and June 2023. MRI was performed using 3-Tesla scanners. The ICP sign was deemed positive when the bilateral ICP signal intensity exceeded that of the medulla oblongata on axial FLAIR images. MCP and HCB signs were also evaluated. Two independent neuroradiologists evaluated all MRIs, and interobserver agreement was assessed using Kappa statistics. Univariable and multivariable logistic regression analyses identified predictive features and diagnostic performance was assessed.

RESULTS: The ICP sign was more prevalent in patients with MSA-C (65%) compared to those with SCA (6.9%; $P < .001$). HCB and MCP signs were more frequent in patients with MSA-C (n = 110 and n = 134) than in those with SCA (n = 19 and n = 30; $P<.001$). The ICP sign demonstrated the highest specificity (95%) for predicting MSA-C, with an AUC of 0.82, respectively. The MCP sign exhibited superior sensitivity (87%) but lower specificity and AUC compared to the ICP sign. Combining the ICP and MCP signs improved the AUC to 0.86. Integrating clinical features (age, sex, and disease duration) with imaging features yielded excellent diagnostic performance, with an AUC of 0.98.

CONCLUSIONS: The ICP sign on FLAIR imaging exhibits high specificity in distinguishing MSA-C from SCA. Integrating clinical and imaging features further enhances diagnostic accuracy, potentially improving differential diagnosis in clinical settings of cerebellar ataxia.

ABBREVIATIONS: AUC = area under the curve; HCB = hot cross bun; ICP = inferior cerebellar peduncle; ICI = integrated calibration index; IQR = interquartile range; IRB = Institutional Review Board; MCP = middle cerebellar peduncle; MDS = Movement Disorder Society; MSA = multiple system atrophy; MSA-C = multiple system atrophy with predominant cerebellar ataxia; SCA = spinocerebellar ataxia.

Received month day, year; accepted after revision month day, year.
From the Department of Radiology and Center for Imaging Science (C.Y.L., Y.S., B.S., M.S., S.T.K., E.Y.K.), Samsung Medical Center, Sungkyunkwan University School of Medicine, Seoul, Republic of Korea; Department of Digital Health (S.H.), Samsung Advanced Institute of Health Sciences and Technology (SAIHST), Sungkyunkwan University, Seoul, Republic of Korea; Medical AI Research Center, Research Institute for Future Medicine (S.H.), Samsung Medical Center, Seoul, Republic of Korea; Department of Neurology (J.Y.), Neuroscience Center (J.Y.), Samsung Medical Center, Sungkyunkwan University School of Medicine, Seoul, Republic of Korea.

Disclosure of potential conflicts of interest: None.

Please address correspondence to Eung Yeop Kim, MD, Department of Radiology and Center for Imaging Science, Samsung Medical Center, Sungkyunkwan University School of Medicine, 81 Irwon-ro Gangnam-gu, Seoul 06351, Republic of Korea
Tel: 82-2-3410-1701; Fax: 82-2-3410-0055; E-mail: neuroradkim@gmail.com

SUMMARY SECTION

PREVIOUS LITERATURE: The HCB sign is a characteristic imaging marker of MSA-C, but it can also be present in SCA patients, limiting its diagnostic specificity. The MCP sign has also shown limited utility due to its presence in various conditions and healthy individuals. Previous pathological studies have shown involvement of the ICP in MSA-C, but its potential as a diagnostic marker on conventional MRI remains unexplored.

KEY FINDINGS: The ICP sign demonstrated high specificity (95%) and diagnostic performance (AUC 0.82) for differentiating MSA-C from SCA. Integration of clinical features with imaging markers, including the ICP sign, achieved excellent diagnostic accuracy (AUC 0.98).

KNOWLEDGE ADVANCEMENT: We established the ICP sign as a novel, highly specific imaging marker for MSA-C diagnosis using conventional FLAIR imaging. The integration of this sign with other imaging and clinical features provides a comprehensive diagnostic approach for distinguishing MSA-C from SCA.

INTRODUCTION

In 2022, the Movement Disorder Society (MDS) revised the 2008 consensus criteria for diagnosing multiple system atrophy (MSA), addressing concerns about the original criteria's limited diagnostic sensitivity and accuracy, which hindered potential treatment

opportunities for MSA patients.[1] The updated criteria introduced additional brain MRI markers for diagnosing clinically established and probable MSA, supplementing the existing criteria such as atrophy of putamen and infratentorial structures (pons and middle cerebellar peduncle).[2] The updates include increased putamen diffusivity on diffusion-weighted imaging and the hot cross bun (HCB) sign on T2-weighted images, underscoring the expanded role of MRI biomarkers in diagnosis.[3-7] However, this HCB sign typically appears in later stages of MSA and may also occur in other conditions, posing a challenge in distinguishing MSA with predominant cerebellar ataxia (MSA-C) from spinocerebellar ataxia (SCA)—a crucial differential diagnosis in patients with ataxia, given the similarity of their symptoms; however, the grave prognosis of MSA-C is due to progressive autonomic dysfunction and nigrostriatal symptoms associated with alpha-synucleinopathy.[8-10]

The inferior cerebellar peduncle (ICP) is a bundle of fibers connecting the cerebellum to the medulla oblongata and spinal cord, comprising the restiform and juxtarestiform bodies.[11] Previous autopsy studies have identified ICP as the earliest structures damaged by alpha-synucleinopathy, leading to glial cytoplasmic inclusions and demyelination of affected sites in patients with MSA-C.[12,13] This observation led researchers to hypothesize that ICP hyperintensity on T2 FLAIR MRI images might reflect these pathological alterations, potentially serving as a distinct marker for MSA-C. To investigate this hypothesis, we examined its occurrence in our patient cohort and compared it with patients with SCA used as controls. We also assessed the diagnostic performance of ICP hyperintensity and developed a multivariable prediction model incorporating other known brain MRI markers to distinguish MSA-C from SCAs, aiming for more accurate differentiation between these conditions.

MATERIALS AND METHODS

Patient Selection and Baseline Data Collection

This study was approved by the Institutional Review Board (IRB, 2023-08-001-001). All methods adhered to relevant STARD checklist and regulations, and a waiver of informed consent was granted by the IRB (Online Supplemental Data). Medical records of patients with suspected MSA-C and genetically confirmed SCAs from a single institution were retrospectively reviewed. Between January 2012 to June 2023, 179 patients with MSA-C were initially identified; eventually, 153 patients were included based on the second consensus diagnostic criteria of MSA-C.[1,14] Patients exhibiting a static course, lacking autonomic failure as described in the criteria, or presenting with other explicable causes of cerebellar ataxia were excluded. Furthermore, those who manifested initial symptoms before 50 years of age, SCA panel tests were conducted to exclude the possibility of autosomal dominant cerebellar ataxia.

Regarding SCAs, 80 patients with positive genetic tests visited our center in the same period. Patients in the MSA-C and SCA group were included if their MRI scans were obtained at the onset of symptom. Patients whose MRI findings unavailable or unsuitable for assessment were excluded, resulting in 72 patients with SCAs being included (Fig 1). Baseline characteristics such as sex, age of onset, and disease duration at the time of MRI acquisition were obtained. Disease duration was calculated from the symptom onset, based on medical records, indicating any of the following features: gait disturbance due to imbalance or slowness, dysarthria, hand incoordination, postural dizziness, or syncope; urinary incontinence or retention; erectile dysfunction; dizziness unexplained by otologic problems or postural change; decreased visual acuity; parkinsonism; and dystonia.[15,16]

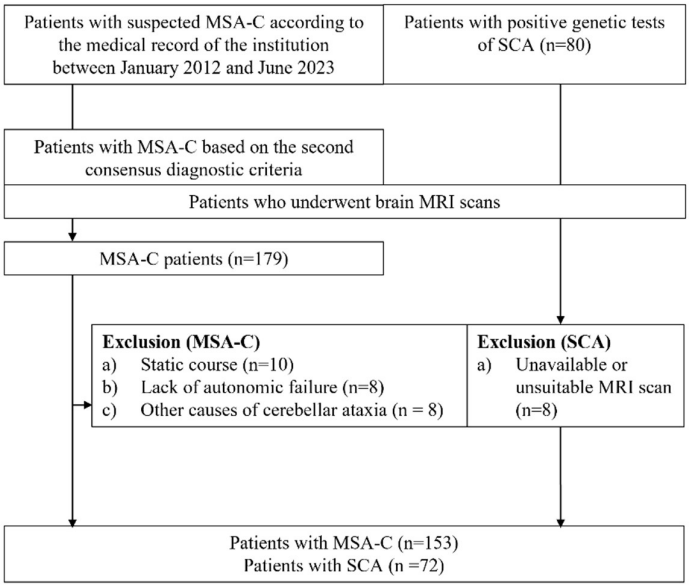

FIG 1. Study flowchart. MSA-C = multiple system atrophy with predominant cerebellar ataxia; SCA = spinocerebellar ataxia.

MRI Acquisition and Analysis

MRI was performed using 3-Tesla scanners (Achieva, Ingenia, Ingenia CX [Philips Medical System, Best, Netherlands], and Genesis

Signa [GE Healthcare, Milwaukee, WI, USA]) with a standard sixteen to sixty-four-channel head coil. Image acquisitions were conducted as follows: (1) axial T2-weighted images (3,000–4,083 ms repetition time, 80–99 ms echo time, echo train length = 15–16, and 5.0 mm thickness); (2) axial T2 fluid-attenuated inversion recovery (FLAIR, 9,000–11,000 ms repetition time, 103.5–125 ms echo time, echo train length = 0–38, and 5.0 mm thickness); (3) sagittal T1 -weighted images (9.9–416 ms repetition time, 4.6–9 ms echo time, echo train length = 16–240, and 5.0 mm thickness).

The ICP sign was considered positive when the signal intensity of the bilateral ICPs was higher than that of the medulla oblongata on axial FLAIR images (Fig 2). The MCP sign was marked as present or absent based on MCP hyperintensity on T2-weighted and FLAIR images (Fig 3).[17-19] The HCB sign was considered present when both horizontal and vertical lines were observed in the pons, whereas the vertical line sign was considered present when observed either as an isolated vertical line or as the vertical component of cruciform hyperintensity in the pons.[20] Cerebellar atrophies were visually evaluated regarding the vermis and hemispheres.[21,22] Two independent neuroradiology specialists (B.S. and C.Y.L.) who were blinded to clinical information evaluated all MRIs. In cases of discrepancy between the two neuroradiologists, the analysis was decided by a consensus between them. The presence of MCP, ICP, HCB and, vertical line signs were assessed on axial FLAIR images. Cerebellar atrophies were assessed on sagittal T1-weighted images.

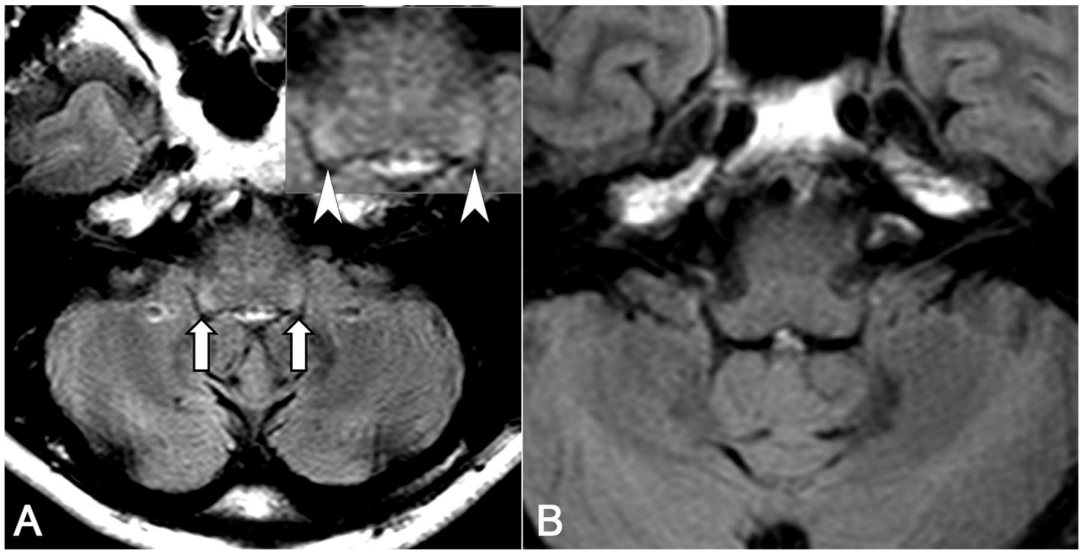

FIG 2. Representative cases of positive/negative inferior cerebellar peduncle (ICP) sign. (*A*) A 45-year-old female presented with cerebellar ataxia. FLAIR image reveals increased signal intensity in the bilateral cerebellar peduncles (arrows; arrowheads in an inset) compared to the medulla. The patient was diagnosed with MSA-C. (*B*) In the T2 FLAIR image of a 48-year-old male diagnosed as spinocerebellar ataxia (SCA), no ICP sign is seen.

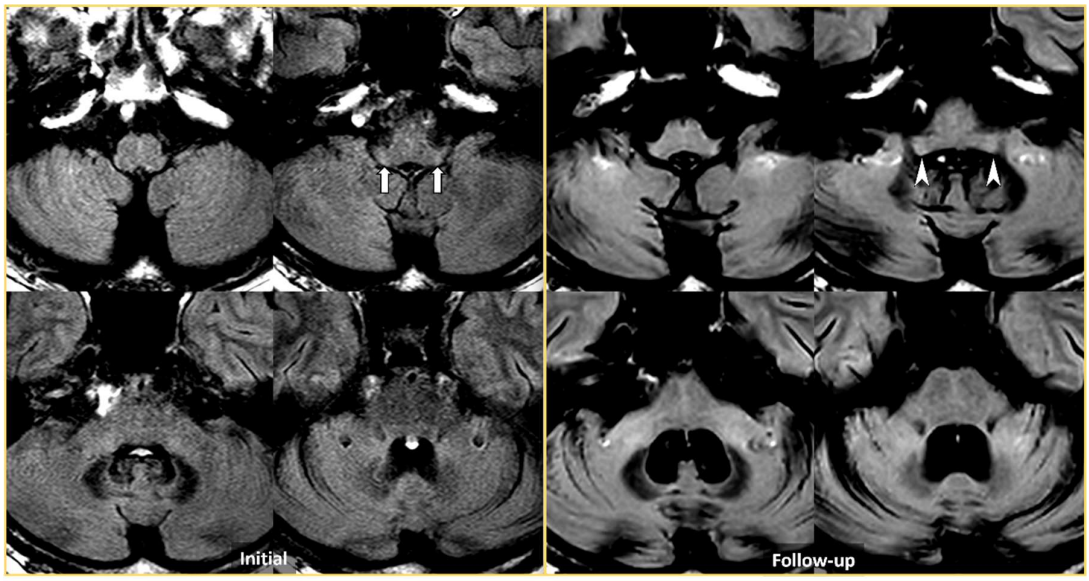

FIG 3. FLAIR imaging in a 53-year-old male who presented with cerebellar ataxia. The initial imaging (left) showed high signal intensity in both inferior cerebellar peduncles (ICPs, arrows), defined as the ICP sign. However, middle cerebellar peduncle (MCP) sign was not evident. On 15-month follow-up MRI (right), the ICP sign was yet again noted (arrowheads) and both the hot

cross bun and MCP signs appeared. The patient was diagnosed as MSA-C. MSA-C = multiple system atrophy with predominant cerebellar ataxia; ICP = inferior cerebellar peduncle.

Statistical Analysis- Development and Assessment of Prediction Model

We explored the complete dataset to identify and select variables for predicting MSA-C. Clinical and imaging features were summarized by median with range or frequency with percentage, depending on variable types and compared between MSA-C and SCA groups using the Student t-, Mann–Whitney U, chi-square, and Fisher's exact tests as appropriate. Interobserver agreement was measured by Kappa statistics. Using features with high predictive values in the exploratory univariable analysis, we underwent multivariable logistic regression, employing a stepwise variable selection using the Akaike Information Criterion. For model development and internal validation, we employed stratified random sampling to divide the dataset into training (70%) and test (30%) cohorts, maintaining balanced proportions of MSA-C and SCA cases in each cohort.

Diagnostic outcomes were evaluated using the area under the receiver operating curves (AUC) with various other measures, including sensitivity, and specificity. Calibration was assessed by drawing calibration plots using a locally weighted scatter plot smoothing curve to illustrate the relationship between the predicted and observed probability of MSA-C. All statistical procedures were performed using R Software (version 4.1.0; R Foundation for Statistical Computing, Vienna, Austria).

RESULTS

Patient Characteristics

Among the 225 patients in our study, 153 (68%) were diagnosed with MSA-C based on the MDS Criteria for the Diagnosis of Multiple System Atrophy, while 72 (32%) were diagnosed with SCA. The SCA group included seven subtypes: SCA1 (4 patients), SCA2 (21 patients), SCA3 (18 patients), SCA5 (11 patients), SCA6 (8 patients), SCA7 (5 patients), and SCA36 (5 patients). The cohort included 124 males (55%) with a median age of 59 years, ranging 19–81 years (Table 1).

Table 1: Demographic characteristics and frequency analysis of MRI findings.

Variables	Total (*n* =225)	MSA-C (*n* =153)	SCA (*n* =72)	*P*-values
Clinical features				
Age[a]	59 (53, 65)	60 (56, 67)	53 (44, 61)	<.001
Disease duration[a,b]	3 (1, 5)	2 (1, 3.3)	5 (2, 11)	<.001
Sex				
Male	124 (55)	79 (52)	45 (63)	.204
Female	101 (45)	74 (48)	27 (38)	
Imaging features				
Scanner				.053
A	182 (81)	119 (78)	63 (88)	
B	6 (2.7)	4 (2.6)	2 (2.8)	
C	36 (16)	30 (20)	6 (8.3)	
D	1 (0.4)	0 (0.0)	1 (1.4)	
ICP sign	105 (47)	100 (65)	5 (6.9)	<.001
HCB sign	129 (57)	110 (72)	19 (26)	<.001
MCP sign	164 (73)	134 (88)	30 (42)	<.001
Cerebellar atrophy	191 (85)	135 (88)	56 (78)	.065
Vertical line	180 (80)	132 (86)	48 (67)	.011

Unless otherwise specified, data are numbers of patients, with percentages in parentheses.
[a]Data are presented as median (1st quartile, 3rd quartile)
[b]Unit of disease duration is a year.
MSA-C, multiple system atrophy with predominantcerebellar ataxia; SCA, spinocerebellar ataxia; ICP, inferior cerebellar peduncle; HCB, hot cross bun; MCP, middle cerebellar peduncle.

The median age at diagnosis differed between the MSA-C and SCA groups, with patients with MSA-C being older (median age 60 years, interquartile range [IQR] 56–67) compared to patients with SCA (median age 53 years, IQR 44–61; $P < .001$). Similarly, disease duration differed; patients with MSA-C had a shorter median disease duration (2 years, IQR 1–3.3) compared to those with SCA (5 years, IQR 2–11; $P < .001$).

In terms of image acquisition, scanner A was the most frequently used in both groups (78% in MSA-C and 88% in SCA), and Fisher's exact test showed no significant difference in scanner distribution between the two groups ($P = .053$). The distribution of sexes across the groups demonstrated no difference ($P = .204$). These patients were divided into training and test cohorts, with baseline characteristics summarized in Online Supplemental Data, Table S1. Both cohorts were balanced for the MSA-C rate and were not

statistically different (all $P > .05$).

Imaging Analysis

Imaging findings of the participants are summarized in Table 1. The presence of the ICP sign was more common in patients with MSA-C (65%, $n = 100$) compared to those with SCA (6.9%, $n = 5$; $P < .001$). All five SCA patients with the ICP sign were of SCA2 subtype. The HCB, MCP and vertical line signs were also more prevalent in patients with MSA-C, occurring in 110 (72%), 34 (88%), and 132 (86%) of cases, respectively, compared to 19 (26%), 30 (42%), and 48 (67%) in patients with SCA ($P < .001$, $P < .001$, and $P = .011$). Cerebellar atrophy was observed in patients with MSA-C (88%, $n = 135$) and those with SCA (78%, $n = 56$; $P = .065$). Interobserver agreements of those findings are summarized in the Online Supplemental Data, Table S2. Except for cerebellar atrophy, other imaging findings exhibited substantial interobserver agreement.

Multiple Logistic Regression Analysis for Predicting the MSA-C

In the multivariable logistic regression analysis, age remained a strong predictor (OR: 1.16, 95% CI: 1.09–1.28, $P < .001$). Disease duration demonstrated an inverse relationship in the multivariable analysis (OR: 0.63, CI: 0.53–0.75, $P < .001$). Among imaging features, the ICP and MCP sign were significant predictors in the multivariable analysis (OR: 32.7, CI: 5.74–186, $P < .001$; OR: 16.8, CI: 5.08–55.8, $P < .001$), highlighting its importance (Table 2).

Table 2: Univariable and multivariable logistic regression analyses for predicting the multiple system atrophy with predominant cerebellar ataxia group.

Variables	Univariable Analysis			Multivariable Analysis		
	OR	95% CI	*P*-value	OR	95% CI	*P*-value
Age	1.10	1.07–1.14	<.001	1.16	1.09–1.28	<.001
Disease duration[a]	0.77	0.70–0.85	<.001	0.63	0.53–0.75	<.001
Sex (Male)	1.58	0.89–2.81	.117			
Scanner (A)[b]	2.02	0.91–4.47	.084			
ICP sign (absence)	25.7	9.78–67.9	<.001	32.7	5.74–186	<.001
HCB sign (absence)	7.31	3.88–13.8	<.001			
MCP sign (absence)	10.4	5.28–20.6	<.001	16.8	5.08–55.8	<.001
Cerebellar atrophy (absence)	2.27	1.07–4.81	.032			
Vertical line (absence)	3.30	1.67–6.54	.001			

[a] Unit of disease duration is a year.
[b]Scanner A (the most frequently used scanner type) is reference, with the odds ratio calculated for other scanner types combined.
The reference category for each variable is presented in parenthesis.
ICP, inferior cerebellar peduncle; HCB, hot cross bun; MCP, middle cerebellar peduncle.

Diagnostic Performance of Imaging and Clinical Features

The diagnostic performance for two significant imaging features, their combinations, the HCB sign, and the integrated imaging and clinical feature (age, sex and disease duration) model are summarized in Table 3 and Fig 4. Among them, ICP sign had the highest specificity (95%), and AUC (0.82, CI: 0.74–0.90) for predicting MSA-C compared to other imaging biomarkers. The MCP sign exhibited the best sensitivity (87%); however, its specificity was less than 50%, with its AUC being lower than that of ICP sign (0.67, CI: 0.55–0.79; $P = .029$). HCB sign demonstrated moderate sensitivity, specificity, and AUC (0.70, CI: 0.58–0.82). When combining ICP and MCP signs, which were independently predictive of MSA-C in the multivariable analysis, its AUC improved to 0.86 (CI: 0.78–0.98), though not different from ICP alone ($P = .114$). When integrating clinical and all evaluated imaging features, it demonstrated excellent diagnostic performance with a sensitivity of 87% and a specificity of 100%. The F1 score was 0.88, and the AUC was notably high at 0.98 (CI: 0.96–1.00), outperforming the ICP sign alone ($P < .001$). In subgroup analysis comparing patients with early (<3 years) and late (≥3 years) disease duration, AUC of the ICP sign did not significantly differ between those two groups (0.83 and 0.77 respectively, P=.187). Notably, in early disease phase, combining the ICP and MCP signs significantly improved diagnostic performance (AUC 0.92) compared to either ICP sign alone ($P < .001$) or MCP sign alone ($P = .005$), achieving both high sensitivity (94%) and specificity (74%, Online Supplemental Data, Table S3).

Table 3: Diagnostic performance of imaging and clinical features for predicting the multiple system atrophy with predominant cerebellar ataxia group.

Parameters	Sensitivity	Specificity	F1-score	AUC[a]	*P*-value[b]

ICP	0.69 [31/45]	0.95 [20/21]	0.73	0.82 (0.74,0.90)	-
MCP	0.87 [39/45]	0.48 [10/21]	0.69	0.67 (0.55,0.79)	.029
HCB	0.69 [31/45]	0.71 [15/21]	0.64	0.70 (0.58,0.82)	.052
ICP+MCP	0.62 [28/45]	0.95 [20/21]	0.70	0.86 (0.78,0.98)	.114
Integrated model[c]	0.87 [39/45]	1.00 [21/21]	0.88	0.98 (0.96,1.00)	<.001

[a]Data in parentheses are 95% CIs with DeLong's test.
[b]*P*-values of AUCs compared with ICP as a reference.
Integrated model includes ICP, MCP sign, age, and disease duration as variables.
ICP, inferior cerebellar peduncle; MCP, middle cerebellar peduncle; HCB, hot cross bun; AUC, area under the curve.
integrated imaging and clinical feature (age, sex and disease duration)

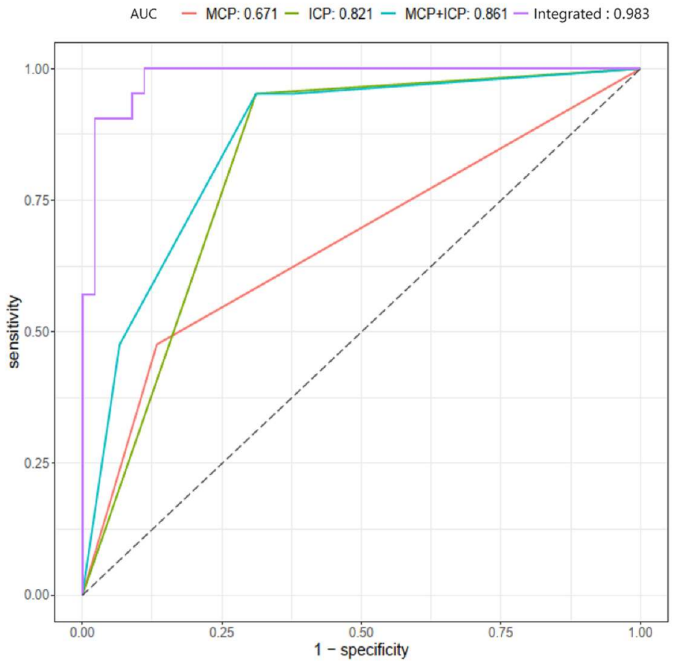

Figure 4. Receiver operating curves of ICP, MCP, combined ICP and MCP signs and the integrated clinicoradiological model for predicting MSA-C. The AUCs of the ICP sign, MCP sign, and combined ICP and MCP signs are 0.82, 0.67, and 0.86, respectively. The integrated model shows the highest AUC of 0.98 with a 95% CI of 0.96–1.00. MSA-C = multiple system atrophy with predominant cerebellar ataxia; ICP = inferior cerebellar peduncle; MCP = middle cerebellar peduncle: AUC = area under the receiver operating curve.

We further assessed the reliability of these imaging predictors and models using the calibration plots and measures (Fig 5). The ICP model showed reliable calibration (intercept = 0.12, slope = 1.25), closely approximating the reference line with a small integrated calibration index (ICI) of 0.03. The MCP model demonstrated systematic underestimation (intercept=-0.13) with over-extreme predictions (slope = 0.71) and increased ICI of 0.61. The combined model (ICP and MCP signs) showed systematic overestimation (intercept = 0.30) with slightly under-extreme predictions (slope = 1.17) and ICI of 0.62. While the integrated imaging and clinical model maintained near-optimal systematic calibration (intercept = 0.02) and the lowest ICI (0.03), its slope (1.74) notably deviated from the reference line, indicating markedly under-extreme predictions.[23,24] The ICP model demonstrates good overall performance with balanced calibration metrics.

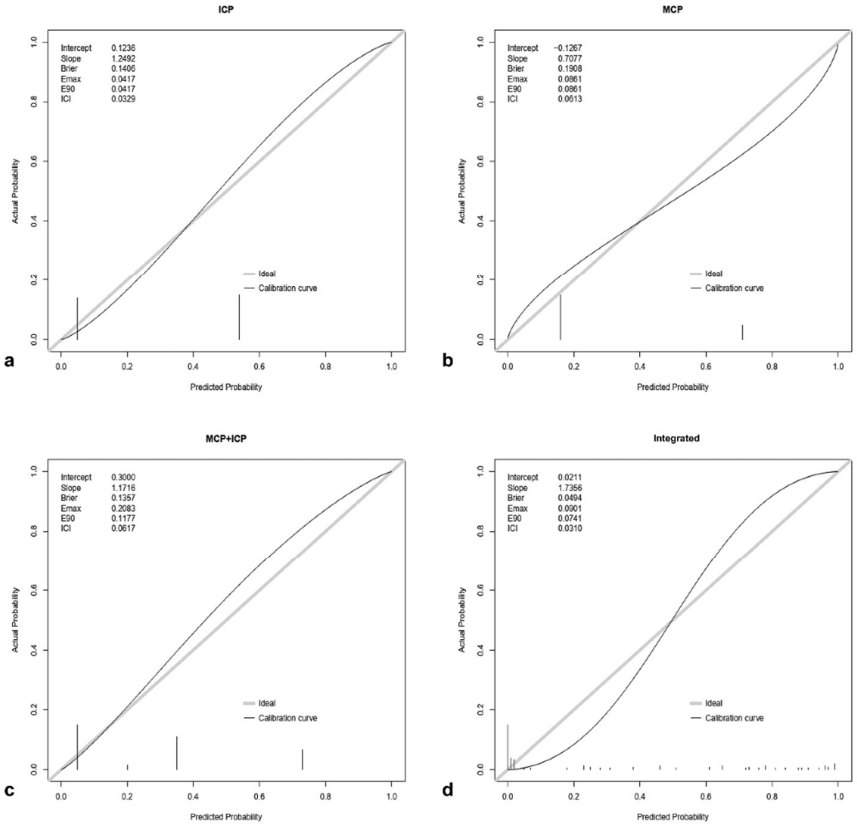

Figure 5. Calibration plots with integrated calibration indices (ICIs) of the ICP, MCP, combined ICP and MCP hyperintensity signs and the integrated clinicoradiological model for predicting MSA-C. Calibration plots comparing ICP sign (intercept=0.12, slope=1.25, ICI = 0.03), MCP sign (intercept = -0.13, slope = 0.71, ICI = 0.61), combined signs (intercept = 0.30, slope = 1.17, ICI = 0.62), and integrated model (intercept = 0.02, slope = 1.74, ICI = 0.03). The ICP sign demonstrates reliable calibration overall. Note. Bars in the calibration plot denote observed outcome frequencies within each bin, reflecting the prediction model's calibration level. Diagonal line indicates perfect calibration. Brier = Brier score (average squared difference in predicted and actual probabilities), Emax/E90/ICI = Maximum/90th quantile/weighted average of absolute difference in predicted and actual calibrated probabilities. ICP, inferior cerebellar peduncle; MCP, middle cerebellar peduncle.

DISCUSSION

Our study revealed that approximately two-thirds of patients with MSA-C exhibited the ICP sign, a rate comparable to that of the HCB sign. While the MCP hyperintensity sign was more common than the ICP sign, it was also observed in over 40% of SCA patients. Previous studies have documented the MCP hyperintensity sign in varying conditions, including healthy individuals, and our research corroborates its presence in a significant proportion of SCA patients.[25,26]

More than a quarter of SCA patients manifested HCB sign in our study. This is consistent with several reports showcasing the presence of HCB sign in SCA patients.[8,27-29] Vertical line sign (also known as the vertical pontine hyperintensity) typically marks the initial stage of the HCB sign and progresses to a complete cruciform hyperintensity in advanced MSA.[20] While Sugiyama et al. found no significant group differences in vertical line sign between MSA-C and SCA3 patients,[30] our larger cohort demonstrated that it could differentiate MSA-C from SCAs. This result may be explained by the greater statistical power of our study.

The diagnostic performance for the ICP sign was the highest among the signs studied, notably for its specificity, which exceeded 95% in our test cohort. This specificity surpassed that of the HCB sign, an imaging biomarker, currently recognized in the MDS consensus criteria for diagnosing MSA-C.[1] The ICP sign's high specificity is particularly valuable given the diagnostic challenges of SCA, which presents similar clinical symptoms and nonspecific imaging findings.[28,31,32] Furthermore, incorporating age and disease duration into our model increased the test AUC to 0.98, marking the first attempt, to our knowledge, to establish an integrated clinicoradiological model.

Studies have demonstrated that 3D-FLAIR sequences enable more detailed visualization of brainstem structures[33] and provide superior lesion detection compared to conventional 2D-FLAIR in various white matter pathologies.[34,35] Future studies employing 3D-FLAIR imaging techniques might further enhance the diagnostic accuracy of ICP assessment in differentiating MSA-C from SCA.

Pathological studies in MSA have revealed pallor or loss of myelin staining in white matter tracts, where glial cytoplasmic inclusions (GCIs)—the diagnostic hallmark of MSA—are frequently observed, particularly in intrafascicular oligodendrocytes.[36] Building upon

these pathological findings, DTI study by Shiga et al. identified decreased fractional anisotropy (FA) of the ICP in half of patients with MSA, encompassing both parkinsonian and cerebellar variants, compared to age-matched controls.[37] Subsequently, Oishi et al., focusing specifically on MSA-C patients, reported reduced FA values in the ICP even during the early stages of the disease.[38] Furthermore, comparative DTI study between MSA-C and SCA1 have demonstrated significant differences in FA values of ICP at the group level.[39] In line with these previous DTI studies, we observed similar ICP abnormalities using T2 FLAIR imaging, and showed a high diagnostic value at the individual level.

As clinically differentiating MSA-C and SCA is challenging especially in the early stage, imaging markers with reliable early diagnostic value are particularly important. Kim et al. reported increased differential value of conventional MRI signs (HCB and MCP hyperintensity) during early disease stages when comparing MSA-C and SCAs.[9] Similarly, our subgroup analysis demonstrated that the ICP sign maintains robust diagnostic performance in both early (<3 years; AUC 0.83) and late disease duration groups (≥3 years; AUC 0.77), with notably high specificity (100%) in the early group.

In our study, the ICP sign was observed in five of 21 patients with genetically confirmed SCA2. Notably, these cases, which represent all false positives in our cohort, tended to have longer disease duration and more prominent brainstem atrophy. Previous studies have described characteristic brainstem involvement in SCA2,[40] with autopsy studies by Estarada et al. showing involvement of the inferior olivary neurons and olivocerebellar fibres,[41] and Yoshii et al. reporting inferior olive hyperintensity on MRI.[42] While our study establishes ICP sign as a useful marker for differentiating MSA-C from SCA, these observations suggest careful consideration may be needed when applying it to cases of advanced SCA2.

Our study has limitations. First, our study did not encompass the full spectrum of diseases in progressive cerebellar ataxia. Given the rarity of conditions such as Sporadic Adult-Onset Ataxia of Unknown Etiology and Idiopathic Late-Onset Cerebellar Ataxia,[43] which are diagnoses of exclusion, these were not included in our cohort. Our primary aim was to differentiate between MSA-C and SCA, the two most prevalent and significant causes of this condition in adults.[43] Second, the retrospective nature of our study may introduce biases, including selection bias and reliance on the quality of historical data. Additionally, the age distribution of patients with MSA-C and those with SCA differed in our cohort. We did not match the ages of these groups, as matching could not fully mitigate this limitation or simulate the conditions of a randomized controlled trial. Moreover, matching would have reduced the number of patients, thereby diminishing the statistical power of our study. Third, we cannot fully elucidate the biological background of the high specificity of ICP sign of MSA-C from SCA. Ataxia-causing lesions in SCA invariably affect the "cerebellar module," which is defined as the reciprocal circuitry between the cerebellar cortex, dentate nuclei, and inferior olivary nuclei. This implies that further biohistopathological studies are needed to explain the high specificity of the ICP sign in MSA, as it cannot be solely attributed to the known gliosis or cell loss in the cerebellar cortex and inferior olivary nuclei.[12,44] Lastly, the analysis of imaging findings was qualitative, relying on the visual assessment of radiological signs. This approach is susceptible to interobserver variability and may lack the precision of quantitative imaging analyses, potentially affecting the reproducibility and objectivity of our results.

Despite these limitations, our research offers significant potential benefits for patients with late-onset progressive ataxia in movement disorder clinics, offering insights that may enhance diagnostic accuracy and thereby inform potential treatment strategies.

CONCLUSIONS

In summary, we identified a new complementary imaging biomarker for MSA-C—hyperintensity of the ICP on FLAIR imaging—that reflects the pathological alterations in MSA-C. We demonstrated its diagnostic utility both as a standalone marker and in combination with other imaging biomarkers and clinical features for differentiating MSA-C from SCA.

ACKNOWLEDGMENTS

This research was supported by a grant from the Korea Health Technology R&D Project through the Korea Health Industry Development Institute, funded by the Ministry of Health & Welfare, Republic of Korea (grant number: RS-2023-00266288).

REFERENCES

1. Wenning GK, Stankovic I, Vignatelli L, et al. **The Movement Disorder Society Criteria for the Diagnosis of Multiple System Atrophy**. *Mov Disord* 2022;37:1131-48
2. Schrag A, Good CD, Miszkiel K, et al. **Differentiation of atypical parkinsonian syndromes with routine MRI**. *Neurology* 2000;54:697-702
3. Schrag A, Kingsley D, Phatouros C, et al. **Clinical usefulness of magnetic resonance imaging in multiple system atrophy**. *J Neurol Neurosurg Psychiatry* 1998;65:65-71
4. Baudrexel S, Seifried C, Penndorf B, et al. **The value of putaminal diffusion imaging versus 18-fluorodeoxyglucose positron emission tomography for the differential diagnosis of the Parkinson variant of multiple system atrophy**. *Mov Disord* 2014;29:380-7
5. Krismer F, Beliveau V, Seppi K, et al. **Automated Analysis of Diffusion-Weighted Magnetic Resonance Imaging for the Differential Diagnosis of Multiple System Atrophy from Parkinson's Disease**. *Mov Disord* 2021;36:241-45
6. Kim HJ, Jeon B, Fung VSC. **Role of Magnetic Resonance Imaging in the Diagnosis of Multiple System Atrophy**.

Mov Disord Clin Pract 2017;4:12-20

7. Bajaj S, Krismer F, Palma JA, et al. **Diffusion-weighted MRI distinguishes Parkinson disease from the parkinsonian variant of multiple system atrophy: A systematic review and meta-analysis**. *PLoS One* 2017;12:e0189897
8. Burk K, Skalej M, Dichgans J. **Pontine MRI hyperintensities ("the cross sign") are not pathognomonic for multiple system atrophy (MSA)**. *Mov Disord* 2001;16:535
9. Kim M, Ahn JH, Cho Y, et al. **Differential value of brain magnetic resonance imaging in multiple system atrophy cerebellar phenotype and spinocerebellar ataxias**. *Sci Rep* 2019;9:17329
10. Nishida K, Futamura N. **Hot Cross Bun Sign in Bilateral Middle Cerebellar Peduncle Infarction**. *Stroke* 2023;54:e163-e64
11. George P, Huang XF. *Atlas of the Human Brainstem*: Elsevier;2013
12. Wenning GK, Tison F, Ben Shlomo Y, et al. **Multiple system atrophy: a review of 203 pathologically proven cases**. *Mov Disord* 1997;12:133-47
13. Brettschneider J, Irwin DJ, Boluda S, et al. **Progression of alpha-synuclein pathology in multiple system atrophy of the cerebellar type**. *Neuropathol Appl Neurobiol* 2017;43:315-29
14. Gilman S, Wenning GK, Low PA, et al. **Second consensus statement on the diagnosis of multiple system atrophy**. *Neurology* 2008;71:670-6
15. Luo L, Wang J, Lo RY, et al. **The Initial Symptom and Motor Progression in Spinocerebellar Ataxias**. *Cerebellum* 2017;16:615-22
16. McKay JH, Cheshire WP. **First symptoms in multiple system atrophy**. *Clin Auton Res* 2018;28:215-21
17. Savoiardo M, Strada L, Girotti F, et al. **Olivopontocerebellar atrophy: MR diagnosis and relationship to multisystem atrophy**. *Radiology* 1990;174:693-6
18. Schulz JB, Klockgether T, Petersen D, et al. **Multiple system atrophy: natural history, MRI morphology, and dopamine receptor imaging with 123IBZM-SPECT**. *J Neurol Neurosurg Psychiatry* 1994;57:1047-56
19. Carre G, Dietemann JL, Gebus O, et al. **Brain MRI of multiple system atrophy of cerebellar type: a prospective study with implications for diagnosis criteria**. *J Neurol* 2020;267:1269-77
20. Horimoto Y, Aiba I, Yasuda T, et al. **Longitudinal MRI study of multiple system atrophy - when do the findings appear, and what is the course?** *J Neurol* 2002;249:847-54
21. Nabatame H, Fukuyama H, Akiguchi I, et al. **Spinocerebellar degeneration: qualitative and quantitative MR analysis of atrophy**. *J Comput Assist Tomogr* 1988;12:298-303
22. Klockgether T, Schroth G, Diener HC, et al. **Idiopathic cerebellar ataxia of late onset: natural history and MRI morphology**. *J Neurol Neurosurg Psychiatry* 1990;53:297-305
23. Van Calster B, Nieboer D, Vergouwe Y, et al. **A calibration hierarchy for risk models was defined: from utopia to empirical data**. *J Clin Epidemiol* 2016;74:167-76
24. Van Calster B, McLernon DJ, van Smeden M, et al. **Calibration: the Achilles heel of predictive analytics**. *BMC Med* 2019;17:230
25. Okamoto K, Tokiguchi S, Furusawa T, et al. **MR features of diseases involving bilateral middle cerebellar peduncles**. *AJNR Am J Neuroradiol* 2003;24:1946-54
26. Ngai S, Tang YM, Du L, et al. **Hyperintensity of the middle cerebellar peduncles on fluid-attenuated inversion recovery imaging: variation with age and implications for the diagnosis of multiple system atrophy**. *AJNR Am J Neuroradiol* 2006;27:2146-8
27. Lee YC, Liu CS, Wu HM, et al. **The 'hot cross bun' sign in the patients with spinocerebellar ataxia**. *Eur J Neurol* 2009;16:513-6
28. Meira AT, Arruda WO, Ono SE, et al. **Neuroradiological Findings in the Spinocerebellar Ataxias**. *Tremor Other Hyperkinet Mov (N Y)* 2019;9
29. Way C, Pettersson D, Hiller A. **The 'Hot Cross Bun' Sign Is Not Always Multiple System Atrophy: Etiologies of 11 Cases**. *J Mov Disord* 2019;12:27-30
30. Sugiyama A, Yokota H, Yamanaka Y, et al. **Vertical pons hyperintensity and hot cross bun sign in cerebellar-type multiple system atrophy and spinocerebellar ataxia type 3**. *BMC Neurol* 2020;20:157
31. Furtado S, Payami H, Lockhart PJ, et al. **Profile of families with parkinsonism-predominant spinocerebellar ataxia type 2 (SCA2)**. *Mov Disord* 2004;19:622-9
32. De Joanna G, De Rosa A, Salvatore E, et al. **Autonomic nervous system abnormalities in spinocerebellar ataxia type 2: a cardiovascular neurophysiologic study**. *J Neurol Sci* 2008;275:60-3
33. Kitajima M, Hirai T, Shigematsu Y, et al. **Comparison of 3D FLAIR, 2D FLAIR, and 2D T2-weighted MR imaging of brain stem anatomy**. *AJNR Am J Neuroradiol* 2012;33:922-7
34. Tawfik AI, Kamr WH. **Diagnostic value of 3D-FLAIR magnetic resonance sequence in detection of white matter brain lesions in multiple sclerosis**. *Egypt J Radiol Nucl Med* 2020;51:1-9
35. de Graaf WL, Zwanenburg JJ, Visser F, et al. **Lesion detection at seven Tesla in multiple sclerosis using magnetisation prepared 3D-FLAIR and 3D-DIR**. *Eur Radiol* 2012;22:221-31

36. Papp MI, Kahn JE, Lantos PL. **Glial cytoplasmic inclusions in the CNS of patients with multiple system atrophy (striatonigral degeneration, olivopontocerebellar atrophy and Shy-Drager syndrome)**. *J Neurol Sci* 1989;94:79-100

37. Shiga K, Yamada K, Yoshikawa K, et al. **Local tissue anisotropy decreases in cerebellopetal fibers and pyramidal tract in multiple system atrophy**. *J Neurol* 2005;252:589-96

38. Oishi K, Konishi J, Mori S, et al. **Reduced fractional anisotropy in early-stage cerebellar variant of multiple system atrophy**. *J Neuroimaging* 2009;19:127-31

39. Prakash N, Hageman N, Hua X, et al. **Patterns of fractional anisotropy changes in white matter of cerebellar peduncles distinguish spinocerebellar ataxia-1 from multiple system atrophy and other ataxia syndromes**. *NeuroImage* 2009;47:T72-T81

40. Klockgether T, Skalej M, Wedekind D, et al. **Autosomal dominant cerebellar ataxia type I. MRI-based volumetry of posterior fossa structures and basal ganglia in spinocerebellar ataxia types 1, 2 and 3**. *Brain* 1998;121 (Pt 9):1687-93

41. Estrada R, Galarraga J, Orozco G, et al. **Spinocerebellar ataxia 2 (SCA2): morphometric analyses in 11 autopsies**. *Acta Neuropathol*. 1999;97:306-10

42. Yoshii F, Tomiyasu H, Watanabe R, et al. **MRI signal abnormalities of the inferior olivary nuclei in spinocerebellar ataxia type 2**. *Case Rep. Neurol*. 2017;9:267-71

43. Kim JS, Kwon S, Ki CS, et al. **The Etiologies of Chronic Progressive Cerebellar Ataxia in a Korean Population**. *J Clin Neurol* 2018;14:374-80

44. Koeppen AH. **The pathogenesis of spinocerebellar ataxia**. *Cerebellum* 2005;4:62-73

SUPPLEMENTAL FILES

Supplementary Table 1: Demographic characteristics and frequency analysis of MRI findings in the training and test cohorts

Variables	Total (*n* = 225)	Training cohort (*n* =159)	Test cohort (*n* = 66)	*P*-values
Clinical features				
Age[a]	59 [53, 65]	59 [52, 65]	59 [55, 66]	.289
Disease duration[a,b]	3 [1, 5]	2 [1, 5]	3 [2, 5]	.248
Sex				.740
Male	124 (55)	86 (54)	38 (58)	
Female	101 (45)	73 (46)	28 (43)	
MSA-C[c]	153 (68)	108 (68)	45 (68)	1.000
Imaging features				
Scanner				.678
A	182 (81)	126 (80)	56 (85)	
B	6 (2.7)	4 (2.5)	2 (3.0)	
C	36 (16)	28 (18)	8 (12)	
D	1 (0.4)	1 (0.6)	0 (0.0)	
ICP sign	105 (47)	73 (46)	32 (49)	.837
HCB sign	96 (43)	67 (42)	29 (44)	.92
MCP sign	129 (57)	92 (58)	37 (56)	.646
Cerebellar atrophy	61 (27)	45 (28)	16 (24)	.547
Vertical line	164 (73)	114 (72)	50 (76)	.534

Unless otherwise specified, data are numbers of patients, with percentages in parentheses.

[a]Data are presented as median (1st quartile, 3rd quartile)

[b]Unit of disease duration is a year.

[c]Participants other than MSA-C are SCA.

MSA-C, multiple system atrophy with predominantcerebellar ataxia; SCA, spinocerebellar ataxia; ICP, inferior cerebellar peduncle; HCB, hot cross bun; MCP, middle cerebellar peduncle.

Supplementary Table 2: Interobserver agreement for MRI features

Variables	Kappa Values
ICP sign	0.77 (0.69, 0.85)
HCB sign	0.82 (0.75, 0.90)
MCP sign	0.79 (0.70, 0.88)
Cerebellar atrophy	0.69 (0.55, 0.83)
Vertical line sign	0.77 (0.67, 0.87)

Note: The CI is indicated in parentheses for Kappa.

ICP, inferior cerebellar peduncle; HCB, hot cross bun; MCP, middle cerebellar peduncle

Supplementary Table 3: Diagnostic Performance of Brain MRI Signs by Disease Duration

Disease Duration	Total (MSA-C/SCA)	Sign	Sensitivity (%)	Specificity (%)	AUC	*P*-value[a]
Early (<3 years)	111 (92/19)	ICP	66	100	0.83	-
		MCP	87	48	0.82	.836
		HCB	69	71	0.75	.143
		ICP+MCP	94	74	0.92	<.001
Late (≥3 years)	114 (61/53)	ICP	64	91	0.77	-
		MCP	87	49	0.68	.047
		HCB	69	71	0.73	.267
		ICP+MCP	64	91	0.81	.198

Note: Unlike the main analysis, train-test splitting was not performed for this subgroup analysis to ensure sufficient sample sizes in each disease duration group for reliable statistical comparison.

[a] P-values from DeLong's test comparing AUCs with ICP sign as reference within each disease duration group.

AUC = area under the curve; MSA-C = multiple system atrophy cerebellar type; SCA = spinocerebellar ataxia; ICP = inferior cerebellar peduncle; MCP = middle cerebellar peduncle; HCB = hot cross bx`un.